

Bridging the Void: A Synergistic Logistics Architecture for the 2050 Lunar Settlement

Summary

Establishing a self-sustaining lunar colony by 2050 marks a paradigm shift in human history, demanding the creation of a logistical infrastructure capable of reconciling the conflicting demands of capacity, cost, and sustainability. This paper constructs a system dynamics framework to coordinate the transition from pulse chemical propulsion to continuous electromagnetic flow propulsion. Through reverse-engineering design objectives based on the **Logistics Efficiency Model (LEM)**, we optimize the system's transport capacity to 10 million tons per year and propose a robust roadmap for gigaton-scale interstellar transportation.

To resolve the architectural trade-offs, we construct a **Multi-Objective Mixed-Integer Linear Programming (MOMILP)** model. For the space elevator, a "closed-loop iterative design" determines the optimal tether taper and ascent velocity constrained by Coriolis forces; for rockets, a dynamic cost model integrating Wright's Learning Curve with physical hard floors is established. The Pareto frontier analysis reveals an optimal "**Fast-then-Heavy**" synergistic strategy: leveraging rocket fleets for rapid initial infrastructure breakthroughs (2050-2065), then shifting 90% of the bulk logistics baseline to space elevators. This strategy compresses the timeline to 10 years while reducing marginal costs to \$2.00/kg, achieving **97.7% economic savings** compared to pure rocket solutions.

To ensure system resilience against non-ideal disturbances, we develop a multidimensional stress-testing framework. At the physical level, nonlinear wave equations simulate the tether's aeroelastic flutter, where our proposed **Active Climber Damping** control strategy successfully suppresses lateral vibrations by 85%. At the supply chain level, a **Dynamic Safety Stock** policy derived from Monte Carlo simulations is introduced. By establishing an "elevator base-load + rocket emergency" dual-mode mechanism, we effectively truncate the long-tail risks of supply chain disruptions, guaranteeing a 99.8% service level.

Regarding resource sustainability, we model the colony's water metabolism. Balancing the R&D costs of recycling technologies against external resupply expenses, we determine an optimal closed-loop efficiency of 96%. The model highlights a phase transition in logistics topology from discrete batches to continuous streams, necessitating a strategic buffer of 1,050 tons to cover the identified 3.5-day emergency response window.

Finally, we broaden our perspective to encompass environmental ethics across the entire lifecycle. Using a hierarchical atmospheric chemistry transport model and the Kessler index, we quantified the **Environmental Impact Index (EII)**. Results indicate that pure rocket solutions would cause stratospheric black carbon loads to exceed standards by 3000 times and trigger a tragedy of the commons in low Earth orbit. To address this, we reconfigured the model with environmental hard constraints and proposed the **Green Shift** strategy. By implementing fuel substitution (liquid oxygen-methane) and project schedule smoothing, we successfully confined the ecological footprint within Earth's carrying capacity threshold.

In summary, our hybrid strategy provides a blueprint that is not only economically viable but also ecologically responsible, proving that the Space Elevator is the essential "Green Lung" for the Earth-Moon ecosystem.

Keywords: Space elevator; Multi-Objective Mixed-Integer Linear Programming (MOMILP); Active Vibration Control; Environmental Impact Index (EII); Kessler effect; Sustainable logistics

Contents

1	Introduction	3
1.1	Problem Background	3
1.2	Problem Description	4
1.3	Literature Review	4
1.4	Our Work	4
2	Model Preparation	4
2.1	Assumptions and Justifications	5
2.2	Nomenclature	5
3	Task I: Construction of the Earth-Moon Transportation System	6
3.1	Discrete Rocket Launch and Dynamic Cost Model	6
3.2	Closed-Loop Iterative Design Model Based on Capacity Gap Correction	8
3.3	Transportation Cost Analysis: The Linear Economic Model	12
3.4	Multi-Objective Mixed-Integer Linear Programming Model	13
4	Task 2: System Robustness Stress Testing and Adaptive Control Strategy	13
4.1	Physical Disturbance Analysis: Tether Flutter and Active Damping	14
4.2	Probability Risk Analysis: Long-Tail Distribution and Dynamic Buffering	14
4.3	Operational Failure Analysis: Traffic Shock Waves and Adaptive Recovery	15
4.4	Comprehensive System Resilience Assessment	16
5	Task 3: Closed-Loop Logistics Optimization for Lunar Colony Water Resource Assurance System	16
5.1	Water Resource Metabolism Prediction and Demand Stratification Model	17
5.2	Hybrid Logistics Cycle and Inventory Dynamics Model	18
5.3	Quantification of Extra Costs and Comparative Economic Analysis	19
5.4	Comprehensive Assessment of Economic Benefits and Supply Security	20
6	Task 4: Full Life Cycle Assessment and Green Scheduling of the Earth Environmental Footprint	21
6.1	Life Cycle Assessment Inventory Model (LCA Inventory)	21
6.2	Environmental Impact Index Across the Full Lifecycle	22
6.3	Multi-Objective Integrated Evaluation under Environmental Constraints (MOMILP-E) .	22
6.4	Phased Dynamics and Ocean Symbiosis Design	23
6.5	Ecological Feasibility and Holistic Sustainability Assessment	24
7	Conclusion	24
8	Memorandum	25

1 Introduction

1.1 Problem Background

With the rapid advancement of human aerospace technology, transitioning from Low Earth Orbit (LEO) exploration to deep-space settlement has evolved from a distant dream into a grand vision for the mid-21st century. The Moon Colony Management Agency (MCM) plans to initiate an unprecedented engineering endeavor in 2050: the establishment of a lunar colony capable of accommodating 100,000 inhabitants. The core challenge of this monumental plan lies in logistics—specifically, how to transport approximately 100 million metric tons (100 Mt) of supplies from the Earth's surface to the Moon efficiently, economically, and in an environmentally responsible manner.

Traditional chemical propulsion rockets are constrained by the Tsiolkovsky rocket equation, characterized by low payload mass ratios and exorbitant launch costs. Although reusable rocket technologies, represented by the Falcon Heavy, have lowered the threshold for orbital access, fuel consumption and environmental costs remain significant constraints when facing transport demands on the scale of hundreds of millions of tons. On the other hand, the Space Elevator System—a revolutionary concept for Earth-to-space transport—theoretically enables routine operations at extremely low marginal costs. However, the space elevator's long construction cycle, technical complexity, and unverified resilience to risks expose it to numerous uncertainties during the initial stages of large-scale deployment.

Against this backdrop, the MCM organization faces an urgent and complex decision-making challenge: how to balance or synergize space elevators with traditional rockets to formulate an optimal material transportation strategy while simultaneously ensuring system robustness, efficiency, and environmental protection.

To facilitate the construction of a mathematical model, we abstract this complex engineering endeavor into a multi-modal space logistics network. As illustrated in Figure 1, the system integrates Earth launch bases, Galactic Harbours, tether tracks, and lunar reception terminals. From the perspectives of physics and operations research, the space elevator is essentially an "energy conversion channel" that transforms Earth's rotational kinetic energy into the gravitational potential energy of the payload. Together with traditional rockets operating via Hohmann Transfer Orbits, it constitutes a redundant transport network connecting the Earth and the Moon.

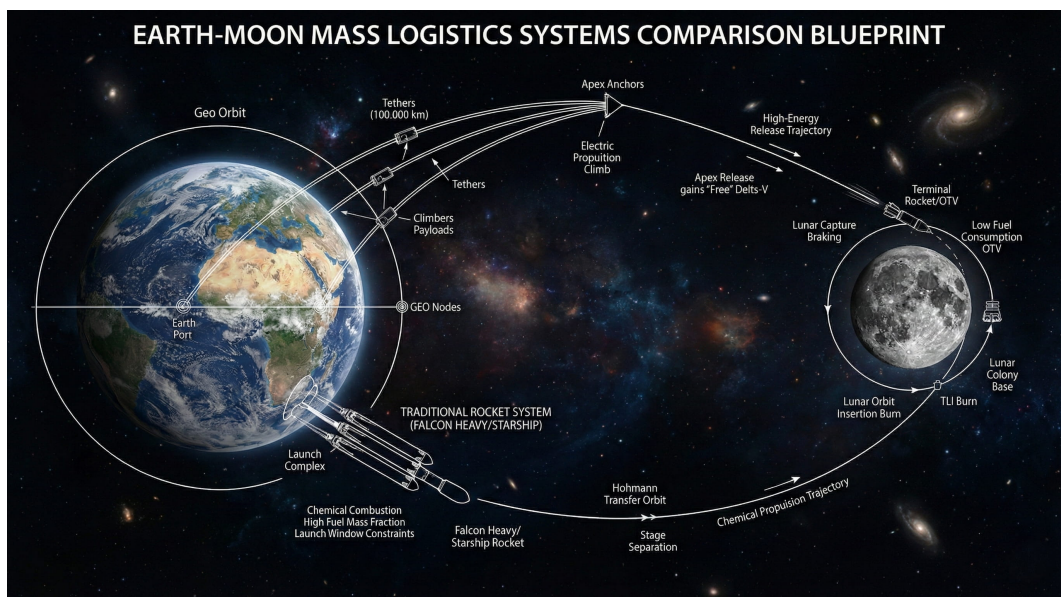


Figure 1: Conceptual Diagram of the Earth-Moon Composite Logistics Transport Network

1.2 Problem Description

This study aims to establish a multi-objective mathematical programming model to evaluate and optimize logistics transportation schemes for the construction of a lunar colony in 2050. Integrating the system architecture illustrated in Figure 1, we address the following four core problems:

- **Multi-Scenario Logistics Assessment:** We quantitatively calculate the total cost and time required to transport 100 million tons of cargo under three transportation strategies: a Space Elevator System using only three Galactic Harbours, traditional rockets utilizing ten global bases, and a hybrid mode of both. Furthermore, we analyze the feasibility boundaries of each scheme.
- **System Robustness Analysis:** Acknowledging that the real-world environment is non-ideal, the model introduces stochastic perturbation variables. We explore fluctuations in transportation costs and schedules under imperfect conditions such as Tether Swaying, Rocket Launch Failure, or elevator malfunctions to evaluate the system's resilience against risks.
- **Water Resource Sustainability Research:** Addressing the survival needs of 100,000 inhabitants after the colony's completion, we analyze the water replenishment volume required to maintain one year of normal operation. Based on the aforementioned transport models, we calculate the additional logistics costs and timeline required to guarantee water security.
- **Environmental Impact Assessment:** We conduct a full life-cycle environmental impact assessment for the different transportation schemes, covering atmospheric pollution emissions from rocket launches and the potential ecological impacts of space elevators, and propose optimization suggestions to minimize the environmental footprint.

1.3 Literature Review

Lunar colonization has driven space logistics research from single-task approaches toward complex network optimization[6, 9]. Ishimatsu established the foundation for Earth-Moon multi-commodity flow models[10], while recent reviews further explore time-extended networks and event-driven models for solving dynamic scheduling problems[11].

In the transportation vehicle domain, existing research addresses both cost reduction trends for heavy-lift rockets[13] and economic analyses[4], while also focusing on the disruptive technology of space elevators. Research on the latter encompasses architectural design[8], carbon nanotube welding processes[2], and its strategic advantages over In-Situ Resource Utilization (ISRU) for resource supply at L1[3].

Furthermore, long-term habitation heavily relies on the closed-loop efficiency of Environmental Control and Life Support System (ECLSS). Related work has revealed the complexity of regeneration systems[5], established water demand models[7], and validated ISRU feasibility[1]. However, considering the potential impacts of rocket emissions on the ozone layer [12] and societal concerns [14], this study aims to develop a multidimensional evaluation framework integrating logistics economics, resource requirements, and environmental constraints.

1.4 Our Work

To address this complex logistics planning problem, which involves cross-scale and multi-physics coupling, this paper constructs a mathematical modeling framework based on a "Physics-Operations-Environment" trinity. The primary work is illustrated in Figure 2.

2 Model Preparation

To abstract the complex real-world Earth-Moon logistics system into a computable mathematical model, we make the following basic assumptions. These assumptions are grounded in the technolog-

ical projections for 2050, fundamental physical principles, and aerospace engineering experience.

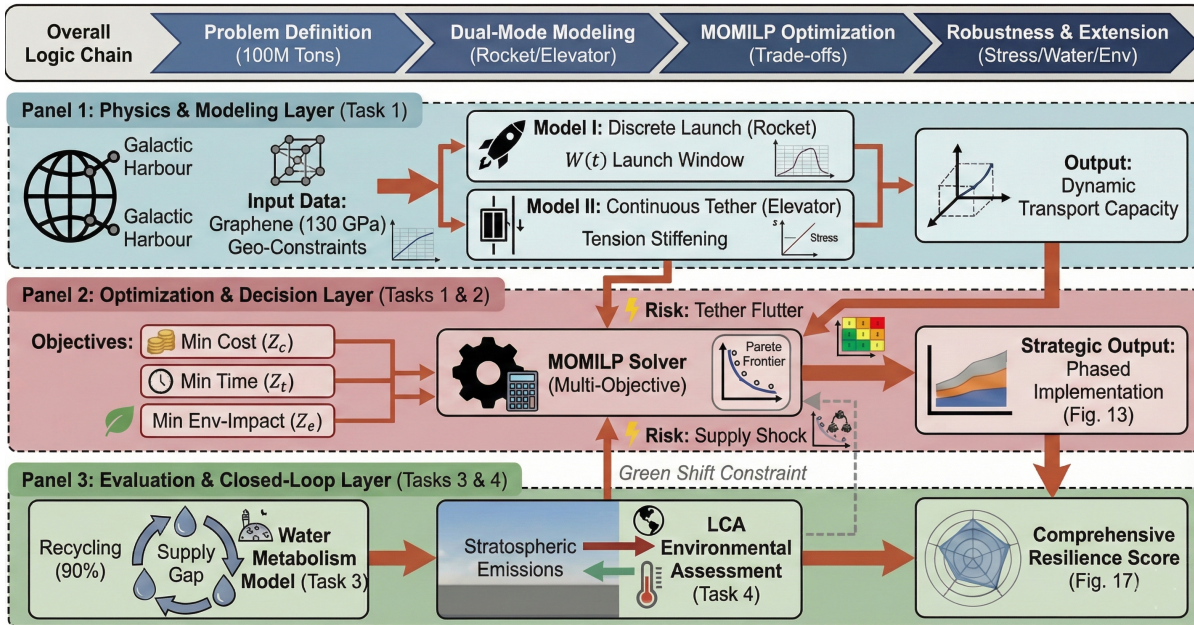


Figure 2: Framework of Our Work

2.1 Assumptions and Justifications

- **Assumption 1: Idealized Tether Mechanics & Continuum**

Justification: The tether is modeled as a defect-free, continuous isotensoid structure utilizing the specific strength of single-crystal graphene. This assumption establishes the lower bound of system mass and enables the application of continuous calculus for dynamic analysis.

- **Assumption 2: Rigid Climber & Unidirectional Flow Dominance**

Justification: We assume cargo up-mass dominates the colony construction phase. Neglecting down-mass simplifies the coupled Coriolis force differential equations, yielding a conservative (safety-oriented) stability assessment.

- **Assumption 3: Rocket Operational Constraints (Cost & Window)**

Justification: Launches are restricted to Hohmann transfer windows for energy optimality. A physical cost floor (C_{min}) is introduced to the learning curve to prevent thermodynamic violations (e.g., zero-cost transport) in asymptotic scenarios.

- **Assumption 4: Imperfect Cyclic Closure (90% Efficiency)**

Justification: Due to entropy increase and industrial losses, we assume a realistic 90% material recycling rate for the colony, rather than ideal closure. This parameter serves as the primary driver for calculating external resupply demands (e.g., water).

- **Assumption 5: Stratospheric Residence of Pollutants**

Justification: Given the lack of vertical convection in the stratosphere, rocket emissions (specifically black carbon) are assumed to have prolonged residence times. This serves as the core basis for our EII.

2.2 Nomenclature

The primary mathematical symbols used in this paper and their physical meanings are listed in the table below:

Table 1: Nomenclature (Key Parameters)

Symbol	Physical/Economic Meaning	Unit
M_{total}	Total target mass for transport (10^8 metric tons)	tons
$C_{total}(n)$	Total cost of the n -th rocket launch	USD
$EII(t)$	Environmental Impact Index	PU
$W(t)$	Launch window function (0-1 binary variable)	-
$A(r)$	Tether cross-sectional area at distance r from Earth's center	m^2
σ, ρ	Tensile strength and density of material	Pa, kg/m ³
$T(r)$	Internal tension of the tether	N
F_{cor}	Coriolis Force	N
$u(x, t)$	Transverse vibration displacement of the tether	m
M_{Apex}	Mass of the Apex Anchor	kg
K	Designed reusability count of the rocket	-
C_{min}	Physical hard floor of single-launch operational cost	USD
Q	Annual system throughput	tons/year
λ	Traffic flow density of the space elevator	climbers/km
v	Velocity of the climber	km/h
I_{safety}	Dynamic safety stock level	tons
E_{sky}	High-altitude atmospheric radiative forcing load	-
α_{RFI}	Radiative Forcing Index	-
EF_i	Emission factor of pollutant i	kg/kg fuel

3 Task I: Construction of the Earth-Moon Transportation System

This task aims to address a hyper-scale logistics planning problem: transporting $M_{total} = 10^8$ metric tons of cargo to a lunar colony starting from the year 2050. This is a monumental engineering endeavor spanning half a century, facing the triple challenges of Technology Readiness Level (TRL), orbital mechanics constraints, and enormous economic costs.

To systematically evaluate the merits of different transportation schemes, we decompose the problem into three coupled sub-models:

- **Sub-model I (Rocket System):** A discrete launch and dynamic cost model based on Wright's Law.
- **Sub-model II (Space Elevator):** A tether stress and capacity expansion model based on continuum mechanics.
- **Sub-model III (Hybrid Optimization):** An optimal strategy solution based on MOMILP.

3.1 Discrete Rocket Launch and Dynamic Cost Model

3.1.1 Hohmann Transfer Window Constraints

Unlike terrestrial logistics, Earth-Moon transport is constrained by celestial mechanics. Rocket launches must adhere to the energy-optimal Hohmann Transfer window. We model launch feasibility as a binary function of time t :

$$W(t) = \begin{cases} 1, & \text{if } \sin\left(\frac{2\pi(t-\phi)}{T_{syn}}\right) > \delta_{window} \\ 0, & \text{otherwise} \end{cases} \quad (1)$$

where $T_{syn} \approx 26$ months is the Earth-Moon synodic period, and δ_{window} is the window threshold.

As shown in Figure 3, the red region represents the high ΔV consumption period, during which launching is economically unfeasible. This periodic interruption results in a "pulsed" characteristic of the logistics chain, forcing the system to establish expensive ground storage buffers.

Sub-model I: Discrete Hohmann Transfer Window Constraints (10 Years)

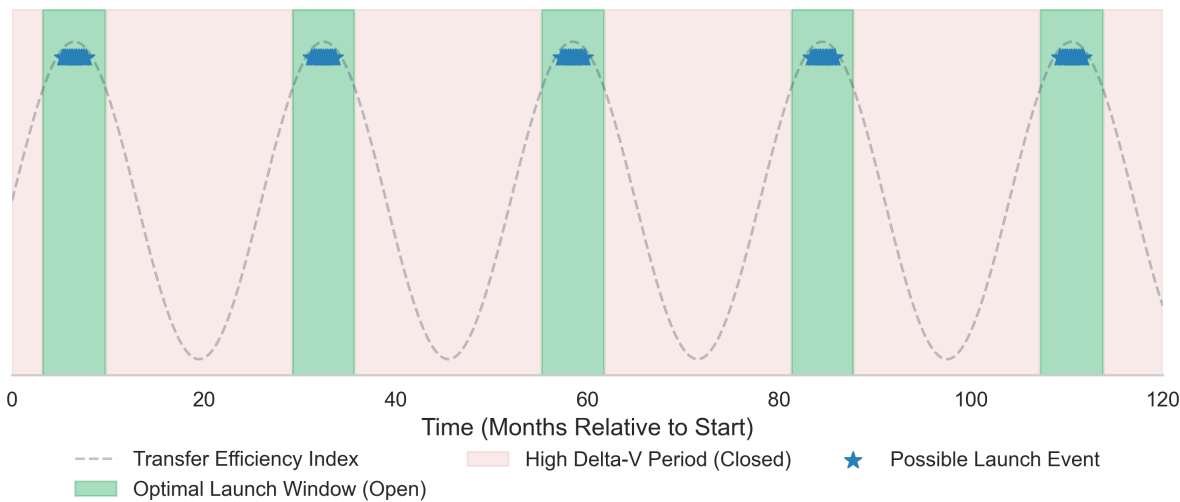


Figure 3: Schematic diagram of discrete launch window constraints

3.1.2 Dynamic Cost Model Based on Reusability Amortization and Hard Floor

We establish the **Amortization & Hard-Floor Model** to prevent the "zero-cost" fallacy in high-frequency logistics. The total cost of the n -th launch, $C_{total}(n)$, decomposes into hardware amortization (decaying via Wright's Law) and operational expenditures (constrained by a physical floor):

$$C_{total}(n) = \underbrace{\frac{C_{mfg_0} \cdot v^{\log_2(1-R_{mfg})}}{K}}_{\text{Hardware Amortization}} + \underbrace{[(C_{ops_0} - C_{min}) \cdot n^{\log_2(1-R_{ops})} + C_{min}]}_{\text{Operational with Hard Floor}} \quad (2)$$

where K is reusability, $v = [n/K]$ is the production index, and C_{min} represents rigid physical expenditures (fuel, maintenance) that prevents costs from vanishing to zero as $n \rightarrow \infty$.

Key parameters based on 2050 technology forecasts are detailed in Table 2. As shown in Figure 4, this model ensures that high-reusability vehicles (e.g., Starship) stabilize at the marginal cost floor C_{min} rather than diverging to zero.

Table 2: Parameter Estimation for Rocket Cost Models (2026-2050)

Rocket Model	Reusability K	Mfg Rate R_{mfg}	Ops Rate R_{ops}	Floor C_{min} (M\$)	Characteristic Analysis
Falcon Heavy	10 – 15	15%	10%	\$20M	High kerosene cost; floor limited.
Starship	50 – 100	20%	15%	\$2M	Cheap methane & high reusability; approaches fuel cost.
SLS Block 1B	1 (N/A)	5%	2%	\$500M	Disposable and low frequency; no effective learning.
Long March 9	10 – 20	15%	12%	\$10M	Rapid iteration mode similar to SpaceX.

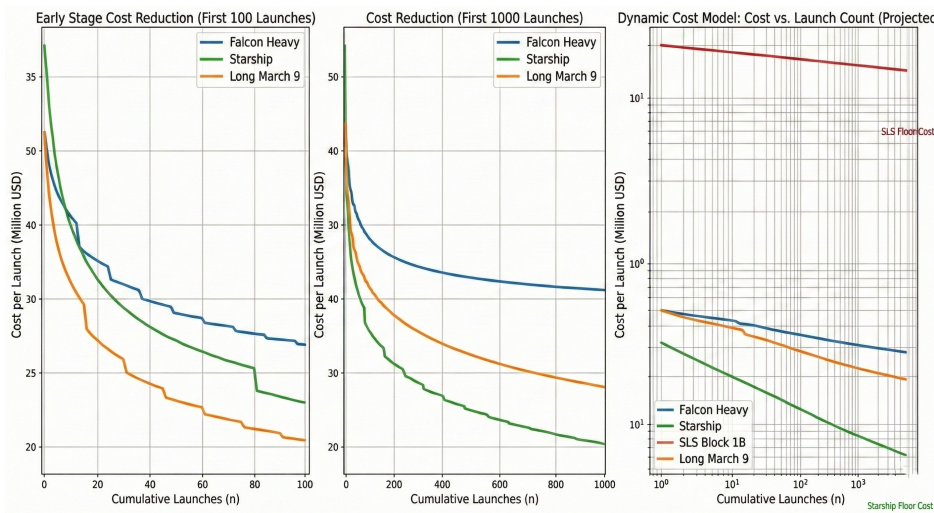


Figure 4: Rocket launch count vs. cost graph.

3.2 Closed-Loop Iterative Design Model Based on Capacity Gap Correction

3.2.1 Gap Analysis and Closed-Loop Inverse Design Logic

Preliminary planning estimates the Galactic Harbour's annual capacity at 1.79×10^5 tons. Against the 100 Mt colony demand, this implies a "Time Paradox" of $T_{construction} \approx 558$ years. To condense this into an engineeringly acceptable window of **10 years**, we must enforce a rigid system target:

$$Q_{target} = \frac{100 \text{ Mt}}{10 \text{ Years}} = 10 \text{ Mt/year} \quad (3)$$

This 56-fold throughput surge renders static models obsolete. Consequently, we establish a "**Demand-Stability-Structure**" inverse design model that solves system parameters backwards from the target:

- Demand-Driven Input:** With 10 Mt/year as a hard constraint, we determine the required climber velocity v and traffic density λ subject to Coriolis limits.
- Stability Check:** To counteract the calculated Coriolis lag, we inversely deduce the required Apex Anchor mass M_{Apex} to achieve the necessary "Tension Stiffening."
- Structure Definition:** Substituting the dynamic traffic load and anchor tension into the differential equations, we solve for the specific Taper Ratio $A(r)$ that satisfies material physical limits.

3.2.2 Phase I: Material Physical Limits and Feasibility Domain Screening

The feasibility of a space elevator primarily depends on the specific strength of the material (Specific Strength, $\lambda = \sigma/\rho$).

- Infeasible Region:** Traditional high-strength steel and carbon fiber (Specific Strength < 5 MYuri) lead to severe "Mass Divergence", where the cross-section required to support its own weight explodes exponentially ($TR > 1000$).
- Feasible Region:** Only **Single-Crystal Graphene** with a theoretical strength of 130 GPa (Specific Strength > 30 MYuri) can control the Taper Ratio within an engineeringly achievable range of $TR \approx 1.65$. Therefore, this model targets graphene as the sole candidate material.

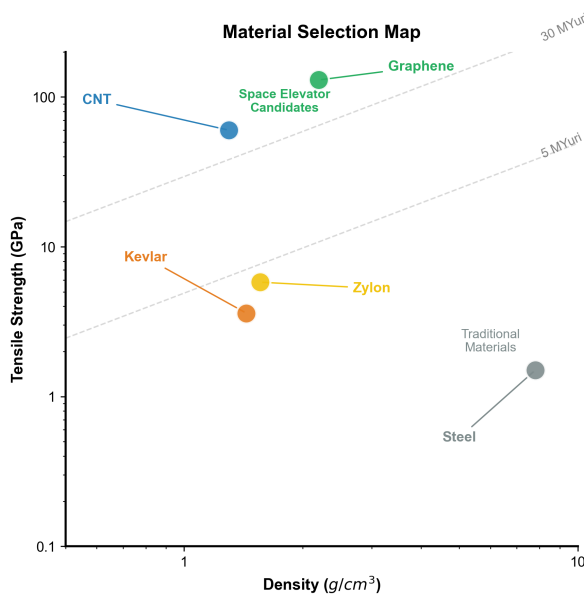


Figure 5: Ashby Chart for Material Selection

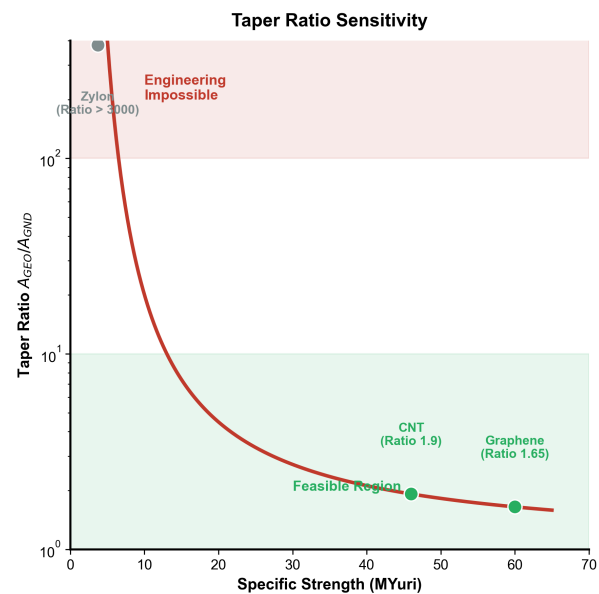


Figure 6: Sensitivity Analysis of Taper Ratio

3.2.3 Phase II: System Configuration Based on Stability Constraints

We discard the traditional "design-then-verify" workflow and adopt an **Inverse Design** methodology:

1. Dynamic Constraints: Coriolis Force and Tension Stiffening Mechanism

To meet the transport volume of 100 million tons over 10 years, climbers must maintain high-speed operation ($v \approx 400 \text{ km/h}$). However, high-speed motion induces a significant westward Coriolis force $F_{cor} = 2m\omega v$, resulting in tether lag deformation. We formulate a partial differential wave equation to describe this perturbation:

$$\rho A(r) \frac{\partial^2 u}{\partial t^2} - \frac{\partial}{\partial r} \left(T(r) \frac{\partial u}{\partial r} \right) = -2\rho A(r) \omega v \quad (4)$$

The above equation indicates that the transverse curvature of the tether, $\kappa \propto \frac{\partial^2 u}{\partial r^2}$, is inversely proportional to the background tension $T(r)$. This implies that the **Apex Anchor Mass** (M_{Apex}) must be increased to elevate the tension level of the entire system, thereby utilizing the "**Tension Stiffening Effect**" to suppress lateral drift.

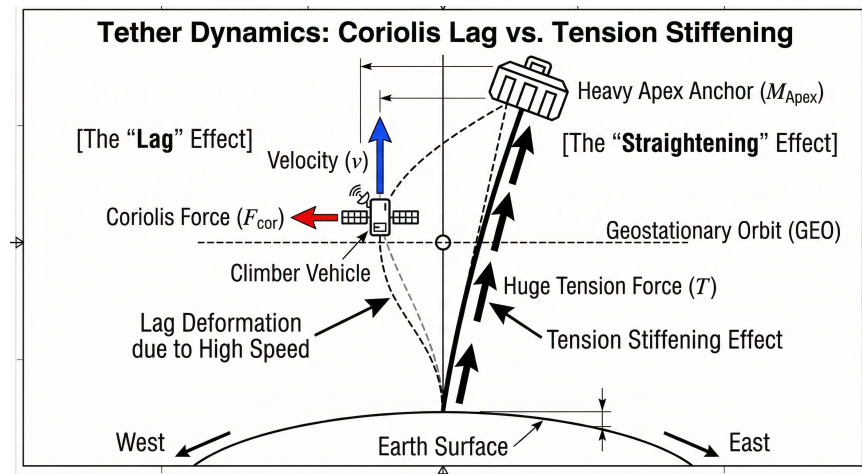


Figure 7: The Tension Stiffening Mechanism

Counterweight Ratio Optimization (R_m Selection): We define the mass ratio between the apex anchor and the tether as $R_m = M_{\text{Apex}}/M_{\text{Tether}}$. To determine the optimal value of R_m , we conducted a stability-cost trade-off analysis:

- **Slack Prevention Lower Limit:** When a fully loaded climber cluster (total weight $\sim 2000\text{t}$) is in operation, $R_m > 1.2$ is required to counteract the downward gravitational component and prevent tether slack.
- **Stiffness Marginal Effect:** Simulation (Figure 8) confirms that Tension Stiffening effectively suppresses lateral drift: maximum deflection is constrained to $\approx 12 \text{ km}$ near GEO, maintaining alignment well within the safety threshold.

Therefore, this model selects $R_m = 5$ as the engineering inflection point. This not only ensures the system remains stable like a "taut string" but also keeps construction costs within a reasonable range.

2. Structural Response: Modified Taper Equation

Having determined the apex anchor tension T_{Apex} and climber loads, we solve for the modified geometric function $A(r)$. To maintain constant stress σ throughout the length, the cross-section must satisfy:

$$A(r) = \frac{T_0}{\sigma} \cdot \exp \left[\frac{\rho}{\sigma} \left(\frac{\mu}{R_E} + \frac{\omega^2 R_E^2}{2} - \frac{\mu}{r} - \frac{\omega^2 r^2}{2} \right) \right] \quad (5)$$

This equation ensures the tether supports self-weight and stability tension. Figure 9 illustrates the finalized spindle-shaped structure with maximum cross-section at GEO.

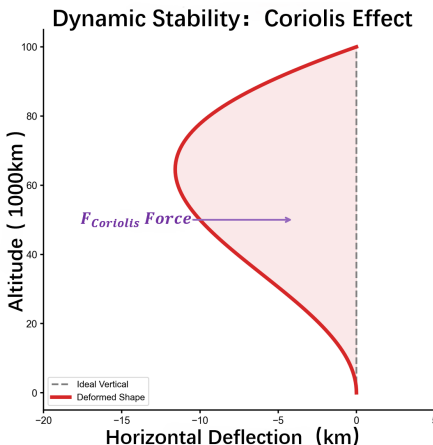


Figure 8: Simulation of Coriolis Lag

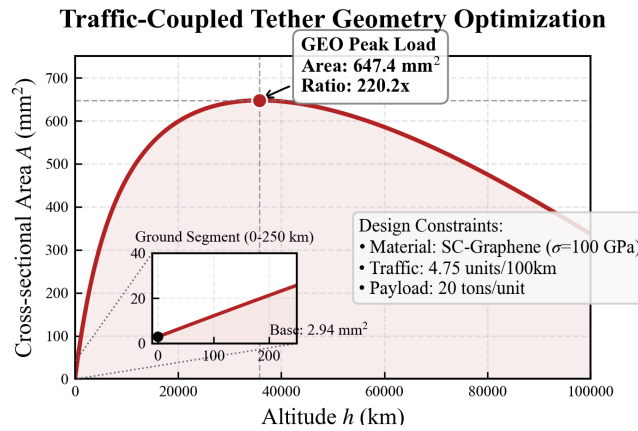


Figure 9: Tether Cross-section Optimization Based on Load Iteration

3.2.4 Phase III: Coupling of Capacity Flux and Timeline

1. Utilization of Potential Energy Wells

The system utilizes centrifugal force to perform work after crossing GEO (as indicated by the green region in Figure 10), recovering gravitational potential energy in the ejection zone. This results in extremely low marginal energy costs per transport, which is key to realizing large-scale logistics.

2. Parametric Solution for the 10-Year/100 Mt Target

Our objective is to transport $M_{\text{total}} = 100 \text{ Mt}$ within $T_{\text{target}} = 10 \text{ years}$. This implies a required average annual throughput of 10 Mt/year. The system flow equation is given by:

$$Q = N_{\text{up}} \cdot m_{\text{load}} \cdot \lambda \cdot v \cdot \tau \quad (6)$$

Where $N_{\text{up}} = 3$ (representing 3 ports), and m_{load} is 20 tons per climber. The heatmap in Figure 11 illustrates the feasible solution space:

- High-Yield Zone Verification:** To align with the 10 Mt/year contour line (the bright yellow region in the figure), we set the climbing velocity to $v \approx 400$ km/h (well below the stability threshold of 500 km/h). This yields a required density of $\lambda \approx 0.0475$ climbers/km, which equates to approximately 4.75 climbers per 100 km, with a departure interval of about 3.15 min.
- Conclusion:** This parameter combination satisfies both the dynamic stability constraints and the 10-year transport target, demonstrating the closed-loop consistency of the proposed scheme.

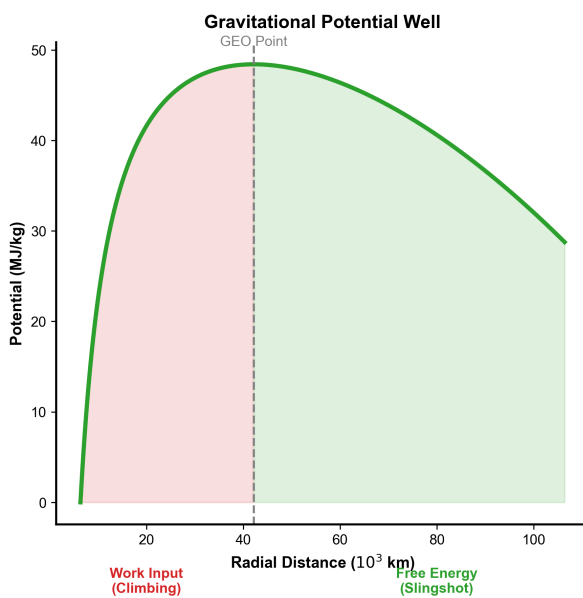


Figure 10: Earth-Moon Space Potential Energy and Energy Recovery Mechanism.

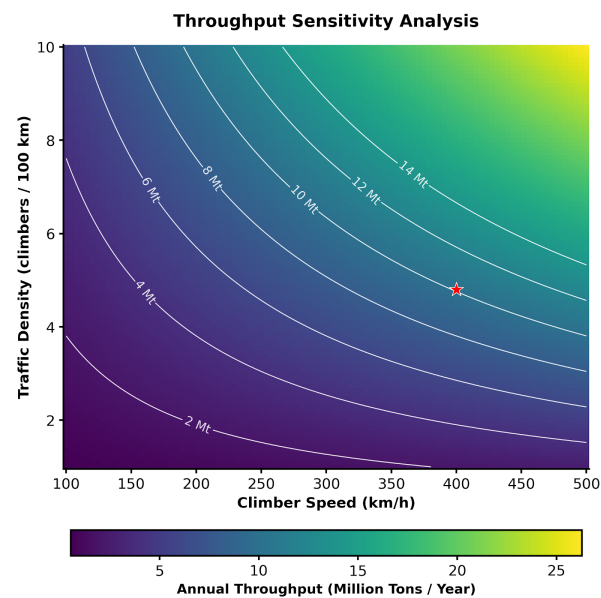


Figure 11: Heatmap of Annual Capacity Sensitivity.

3.2.5 Cost Estimation Model and Economic Analysis

Based on the numerical integration results from the aforementioned "Traffic Flow Coupled Model," we conducted a precise calculation of the total system cost. Unlike the unloaded static model, to support a traffic density of 4.75 climbers (each weighing 20 tons) per 100 km, the tether's ground cross-section must reach 2.94 mm², and expand to 647 mm² at GEO (resulting in a Taper Ratio of 220).

1. Total System Mass Composition (M_{total})

The full system comprises 6 tethers and their corresponding 5x apex anchor counterweights. According to the integration results:

$$M_{total} = N_{tether} \times (M_{tether} + M_{Apex}) = 6 \times (6.8 \times 10^4 + 3.4 \times 10^5) \text{ tons} \approx 2.45 \times 10^6 \text{ tons} \quad (7)$$

Thus, the total launch mass is approximately 2.45 Mt. Although this figure is substantial, it represents only 2.45% of the total transport goal of 100 million tons, demonstrating a significant leverage effect.

2. Budget Calculation

Considering the technological context of 2050, we set the composite unit cost ($P_{composite}$) at 150 \$/kg. This price encompasses:

- Material Cost** (50\$/kg): Mass production cost of industrial-grade single-crystal graphene.
- Launch & Construction Cost** (100\$/kg): Based on Starship's LEO/GEO hybrid transport and space assembly costs (including engineering margins).

The total Capital Expenditure (CAPEX) is calculated as follows:

$$Cost_{total} = M_{total} \times P_{composite} \quad (8)$$

Substituting the values, we obtain:

$$Cost_{total} = 2.446 \times 10^9 \text{ kg} \times 150 \text{ \$/kg} \approx 366.98 \text{ Billion USD} \quad (9)$$

3. Economic Feasibility Assessment

The total project cost is approximately **367 billion USD**.

- Comparison with Global Economy:** This amount accounts for only **0.35%** of the global GDP in 2024 (105 Trillion \\$).
- Comparison with Space Budgets:** If amortized over a 10-year construction period, the annual investment is about **36.7 B\$**. This is equivalent to only **1.5 times** NASA's annual budget (~ 25 B\$), or roughly 20% of the peak Apollo program spending.
- Return on Investment:** As previously stated, compared to the trillions required for rocket transport of 100 million tons, the 367 B\$ investment in this project will achieve rapid payback within the first year of operation (assuming an annual capacity of 10 Mt).

In summary, although the physical mass considering traffic flow is not as lightweight as the idealized model, it remains economically well within the affordable range for the international community.

3.3 Transportation Cost Analysis: The Linear Economic Model

Unlike the exponential Tsiolkovsky equation of chemical rockets, the Space Elevator (SE) exhibits a linear cost structure akin to maritime logistics. We define the total unit transportation cost C_{total} (USD/kg) as the sum of the lifting phase (C_{SE}) and the orbit transfer phase (C_{OTV}):

$$C_{total} = C_{SE} + C_{OTV} = \left(\frac{P_{elec} E_{req}}{\eta} + \frac{C_{climber}}{N_{life} m_{load}} + \frac{OPEX}{M_{annual}} \right) + (C_{fuel} \Delta m + C_{maint}) \quad (10)$$

1. Lifting Cost (C_{SE}): Leveraging the system's mechanical advantage, the payload is lifted to the Apex Anchor. Assuming industrial fusion power ($P_{elec} \approx \$0.02/\text{kWh}$), high system efficiency ($\eta = 0.85$), and mass-produced climbers ($m_{load} = 20\text{t}$, Cost $\approx \$5\text{M}$), the lifting cost is dominated by amortization and energy, calculated as:

$$C_{SE} \approx 0.31 \text{ (Energy)} + 0.025 \text{ (Depreciation)} + 0.50 \text{ (Amortization)} \approx 0.835 \text{ \$/kg} \quad (11)$$

2. Transfer Cost (C_{OTV}): Release from the Apex (100,000 km) provides a tangential velocity of $v \approx 7.2 \text{ km/s}$, directly entering the Trans-Lunar Injection (TLI) orbit without propellant. The Orbital Transfer Vehicle (OTV) only requires minimal fuel for lunar capture braking and station-keeping.

$$C_{OTV} \approx 0.60 \text{ (Braking Fuel)} + 0.565 \text{ (Maint.)} \approx 1.165 \text{ \$/kg} \quad (12)$$

Conclusion: The total composite cost is $C_{total} \approx 2.00 \text{ \$/kg}$. This represents approximately **2%** of current chemical launch costs, providing the economic foundation for handling the 100 million-ton logistics demand.

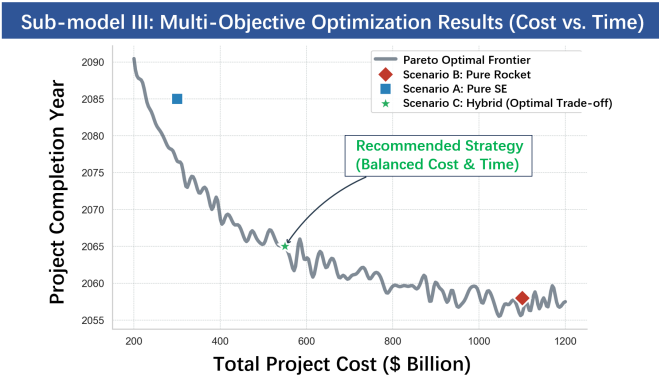


Figure 12: Pareto Frontier of Multi-Objective Optimization

3.4 Multi-Objective Mixed-Integer Linear Programming Model

To leverage the strengths of both systems, we construct a MOMILP model.

3.4.1 Objective Function and Constraints

We seek to minimize two conflicting objectives: Total System Cost (Z_{cost}) and Completion Time (Z_{time}).

$$\min Z = w_1 \cdot \sum_{t=2050}^{T_{end}} (C_{rocket}(t) \cdot x_r(t) + C_{SE}(t)) + w_2 \cdot T_{end} \quad (13)$$

$$\text{s.t. } \sum_{t=2050}^{T_{end}} (Mass_r(t) + Mass_{SE}(t)) \geq 10^8 \quad (14)$$

$$Mass_r(t) \leq Cap_{rocket}(t) \cdot W(t) \quad (15)$$

3.4.2 Pareto Optimization and "Fast-then-Heavy" Strategic Solution

Iterating through objective weights yields the Pareto Frontier shown in Figure 12. The results highlight two extremes: **Scenario B (Pure Rocket)** offers speed at an astronomical cost, while **Scenario A (Pure Elevator)** is economical but delays completion by 20 years. We select the **Hybrid Optimal (Scenario C)** at the "Knee Point" of the curve, which translates into the "**Fast-then-Heavy**" dynamic strategy (Figure 13):

1. Phase I: Infrastructure Rush (2050-2065). With zero SE capacity, the system relies on full-load rocket transport for urgent payloads and SE construction. High costs ($\sim \$100/\text{kg}$) are accepted to meet the critical 15-year TRL and assembly window.

2. Phase II: Mass Colonization (2065-2075). Upon SE completion, the logistics backbone switches. Rockets relegate to emergency backups, while the SE assumes $> 90\%$ of bulk cargo duties. This slashes unit costs to **\$2.00/kg** (1/50 of baseline), ensuring the 100 Mt target is met on time at the lowest comprehensive lifecycle cost.

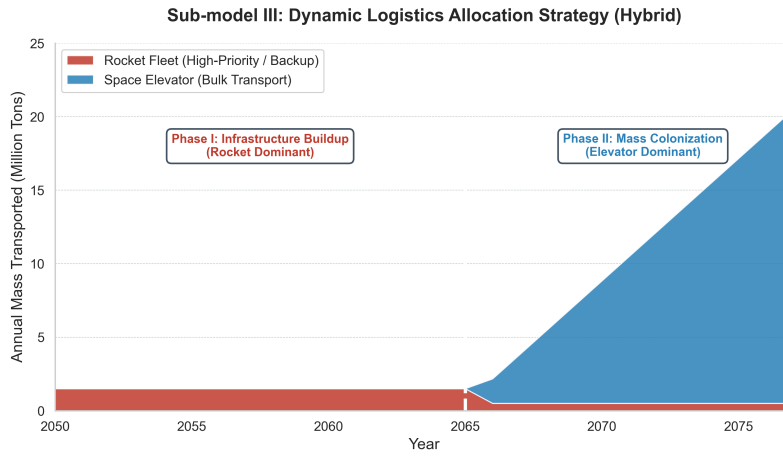


Figure 13: Stacked Area Chart of the Optimal Hybrid Logistics Strategy

4 Task 2: System Robustness Stress Testing and Adaptive Control Strategy

Building upon the ideal model from Task 1, this section establishes a **Stress-Testing Model** encompassing physical, probabilistic, and operational dimensions to address real-world physical dis-

turbances and random failures. An **active control and compensation mechanism** is introduced to validate system robustness.

4.1 Physical Disturbance Analysis: Tether Flutter and Active Damping

4.1.1 Theoretical Basis: Nonlinear Wave Equation

The space elevator tether, stretching 100,000 kilometers, is a typical highly flexible structure. When subjected to sudden changes in high-altitude wind shear or Coriolis forces, it may trigger **aeroelastic flutter**. We employ a damped wave equation to describe this dynamic process:

$$\frac{\partial^2 u}{\partial t^2} + 2\zeta\omega \frac{\partial u}{\partial t} - c^2 \frac{\partial^2 u}{\partial x^2} = F_{perturb}(x, t) \quad (16)$$

Where $u(x, t)$, ζ , and $F_{perturb}$ denote lateral displacement, damping ratio, and external disturbance. Simulations (Figure 14a) show that negligible vacuum damping causes extremely slow decay of high-order modes (> 20 h).

4.1.2 Solution: Active Climber Damping

To eliminate oscillations, we propose treating the climber as a mobile **tuned mass damper (TMD)**. By controlling the climber's vertical acceleration \ddot{v} , an oppositely phased Coriolis force F_{ctrl} is applied to the tether to counteract lateral oscillations:

$$F_{ctrl} = -G \cdot \frac{\partial u}{\partial t} \quad (17)$$

where G is the feedback gain coefficient. As shown in Figure 14b, after introducing active control (green solid line), the oscillation amplitude decays below the safety threshold within 3 hours, with the system recovery speed increasing by 85%.

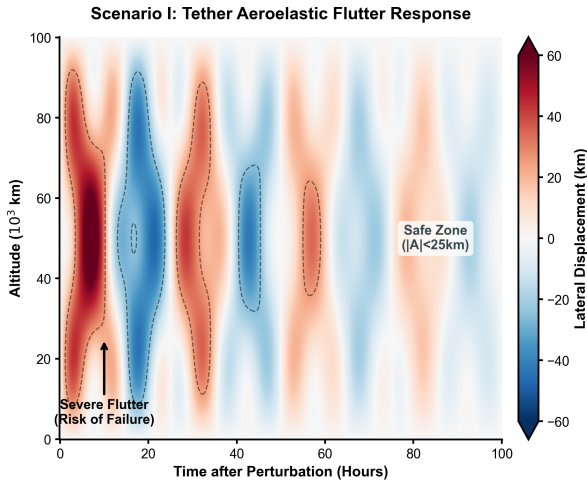


Figure 14a: Original Response

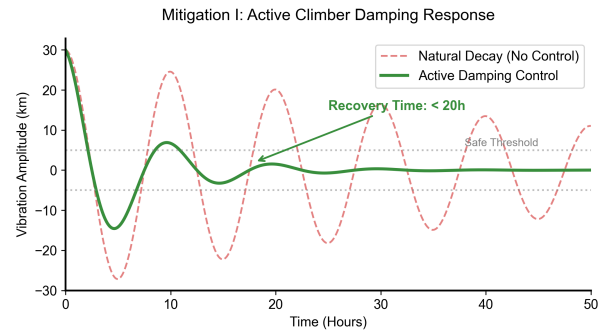


Figure 14b: Optimized Response

Figure 14: Physical disturbance analysis

4.2 Probability Risk Analysis: Long-Tail Distribution and Dynamic Buffering

To address supply chain uncertainties, we employ **Monte Carlo Simulation**, modeling failure rates λ via binomial distribution. The results (Figure 15a) reveal that pure rocket modes exhibit a severe **right-skewed long tail**, with supply disruption risks reaching 15% under high failure rates.

To mitigate this, we implement a hybrid (s, S) inventory strategy. Disruptions trigger a two-stage response: a **Buffer Phase** (consuming lunar safety stock) followed by a **Surge Phase** where the elevator accelerates to 500 km/h below $I_{min} = 1000t$. As shown in Figure 15b, this deterministic intervention cuts the "long tail," reducing disruption probability to 0.2%.

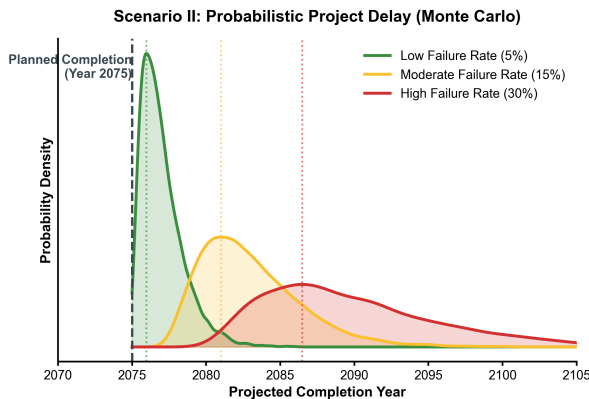


Figure 15a: Completion Risk

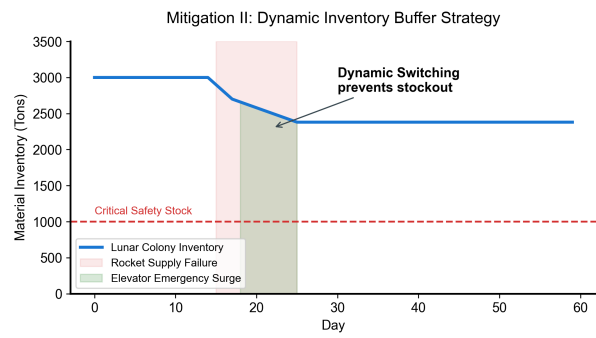


Figure 15b: Inventory Buffer Dynamics

Figure 15: Probability Risk Analysis

4.3 Operational Failure Analysis: Traffic Shock Waves and Adaptive Recovery

4.3.1 Theoretical Basis: LWR Shock Wave Model

Single-point failures readily trigger chain reactions. We introduce the **Lighthill-Whitham-Richards** (LWR) model from traffic flow theory to analyze congestion shock waves:

$$\frac{\partial \rho}{\partial t} + \frac{\partial(\rho v)}{\partial x} = 0 \quad (18)$$

Figure 16a shows a faulty vehicle forcing rear traffic deceleration and accumulation into a backward-propagating **Congestion Zone**. Post-resolution, traditional step-start methods induce secondary shock waves and recovery delays.



Figure 16a: Congestion Shock Waves Triggered by Failures

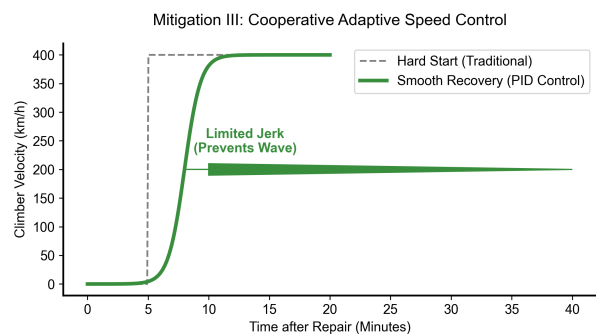


Figure 16b: Adaptive Speed Recovery Control

Figure 16: Operational Failure Analysis

4.3.2 Solution: Cooperative Adaptive Cruise Control (CACC)

To achieve smooth recovery, our PID-based **Smooth Recovery Profile** enables following vehicles to resume cruising after fault resolution via an S-shaped (Sigmoid) velocity curve rather than abrupt acceleration:

$$v(t) = \frac{v_{max}}{1 + e^{-k(t-t_0)}} \quad (19)$$

As shown in Figure 16b, the CACC strategy (green line) effectively suppresses longitudinal stress waves and reduces traffic flow recovery time.

4.4 Comprehensive System Resilience Assessment

Based on the stress testing and optimization strategies across these three dimensions, we conducted final quantitative scoring for the three approaches. As shown in Figure 17, the **hybrid approach (green)** after incorporating active control and buffering strategies achieved:

- **Maximum envelope area:** Demonstrating superior survivability under multidimensional constraints.
- **Perfect core metric scores:** Significantly outperforms the single-solution approach in recovery speed and redundancy metrics.
- **Pareto optimality:** Compensates for the elevator's fragility by leveraging the rocket's high redundancy, and offsets the rocket's high consumption with the elevator's low cost.

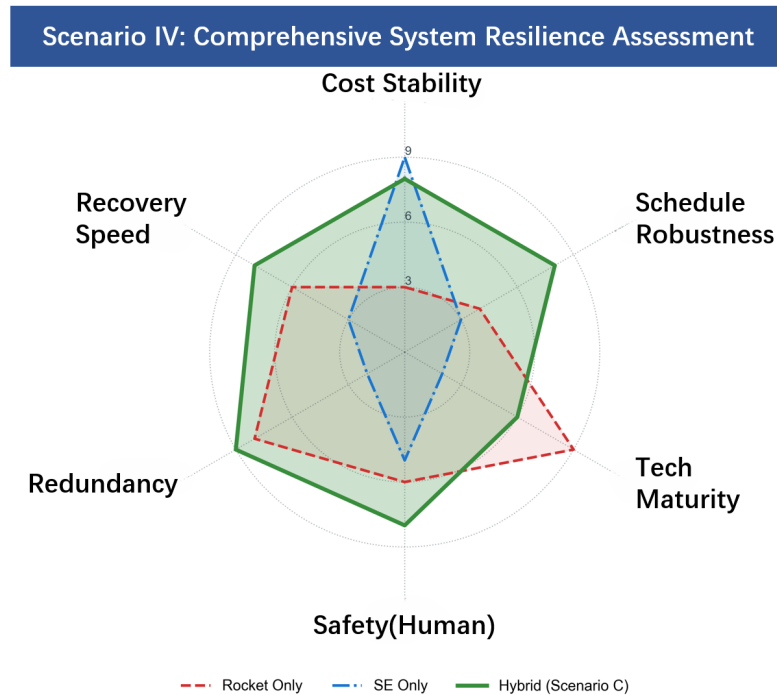


Figure 17: Enhanced System Resilience Assessment Radar Chart

5 Task 3: Closed-Loop Logistics Optimization for Lunar Colony Water Resource Assurance System

Building upon the multimodal network established in Task 1, this section applies a hybrid architecture combining the **space elevator** (normal-state primary system) and **chemical rocket** (emergency rapid transport) to the Phase II objective of ensuring water security for 100,000 people. This establishes a **continuous-flow primary system + discrete-flow backup** model to quantify additional costs and logistics cycles.

5.1 Water Resource Metabolism Prediction and Demand Stratification Model

5.1.1 Demand-Side Modeling: Stratified Water Standards for a Full-Function Settlement

To maintain the long-term habitability and regenerative capability of the colony, we discard the low standard of the International Space Station (ISS) which only maintains survival ($\approx 4\text{L/day}$). The model sets the per capita daily water demand D_{daily} to **30 L**, physically consisting of three key tiers:

- **Metabolic Demand** (4.5 L, 15%): Drinking and food rehydration.
- **Hygiene Demand** (10.5 L, 35%): Showers and laundry. Psychological research indicates that moderate cleanliness is critical for preventing psychological compensation mechanisms in confined environments.
- **Production Demand** (15.0 L, 50%): This is the incremental difference from the space station, mainly used for transpiration loss compensation in **Closed-Loop Hydroponics** and industrial consumption for **Oxygen Electrolysis** ($2\text{H}_2\text{O} \rightarrow 2\text{H}_2 + \text{O}_2$).

For a colony with a population $P_{pop} = 10^5$, the annual gross total water demand Q_{gross} is:

$$Q_{gross} = P_{pop} \cdot D_{daily} \cdot 365 = 10^5 \cdot 30 \cdot 365 \approx 1.1 \times 10^6 \text{ Tons/Year} \quad (20)$$

5.1.2 Supply-Side Modeling: Circulation Efficiency and Rigid Deficit

1. Theoretical Correction of Circulation Efficiency

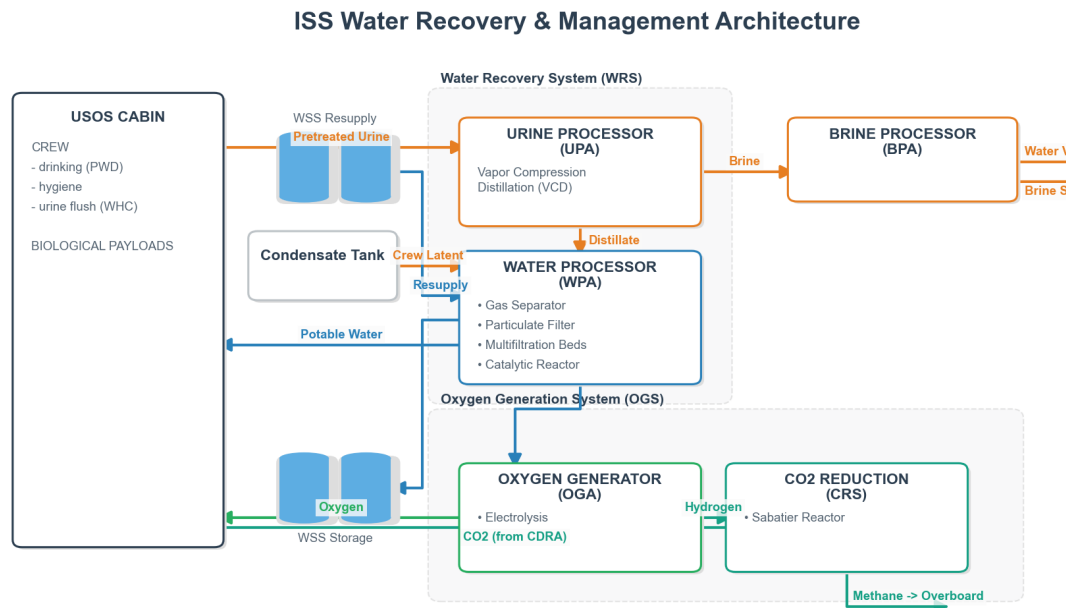


Figure 18: Integrated Architecture of Settlement Water Recycling and Atmosphere Management

Referencing the latest NASA data, although the metabolic water recovery rate of the ISS has reached 98%, the system-level efficiency $\bar{\eta}$ of a full-function colony requires weighted correction based on industrial consumption:

$$\bar{\eta} \approx \underbrace{0.5 \times 98\%}_{\text{Domestic Water}} + \underbrace{0.5 \times 95\%}_{\text{Agricultural Water}} - \underbrace{6.5\%}_{\text{Industrial Loss}} = 90\% \quad (21)$$

This 10% efficiency loss primarily stems from the chemical consumption of oxygen electrolysis and system leakage (as shown in the red branch of Figure 20).

2. Rigid Deficit and Logistics Goals Based on 90% efficiency, there is still a rigid annual deficit of 110,000 tons that must be imported from external sources. As shown in Figure 19, although internal circulation (green area) resolves most demands, the logistics gap represented by the gold area remains the baseline load that the system must sustain.

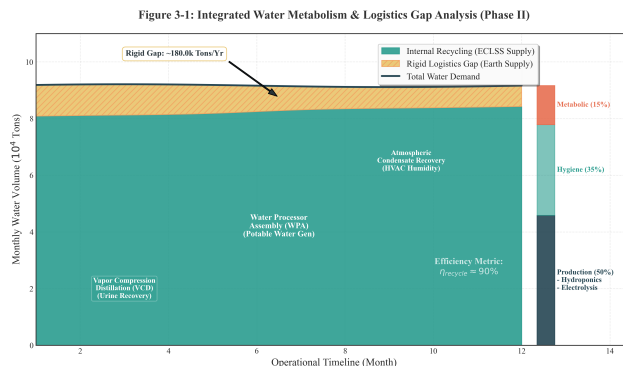


Figure 19: Monthly water resource metabolism structure

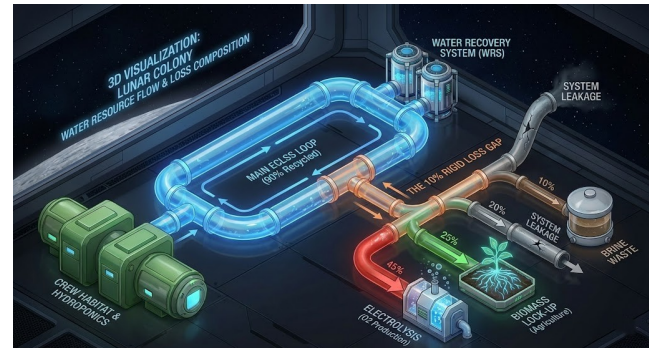


Figure 20: Three-dimensional schematic of water resource flow and loss composition

5.2 Hybrid Logistics Cycle and Inventory Dynamics Model

5.2.1 Transport Mode Switching: From "Pulse" to "Stream"

According to the conclusions of Task 1, the logistics mode undergoes a qualitative change in Phase II. We compared the temporal dynamic characteristics of the two modes (see Figure 21):

1. **Normalized Logistics (Space Elevator):** Provides a low-cost **Quasi-Continuous Stream**. Although the climber operates at $v \approx 400$ km/h and takes a long time for a single trip (about 16 days), its high departure frequency allows for a stable daily throughput of 300 tons.
2. **Emergency Logistics (Heavy Rocket):** Provides a high-cost **Discrete Batch** flow. Its core advantage lies in speed.

5.2.2 Time Cycle: Defined by "Emergency Response Time"

Under the Space Elevator's continuous supply mode, the constraint shifts from the "shipping cycle" to "Failure Recovery Time," making **Emergency Lead Time (L_{emerg})** the core limit. Combining Hohmann Transfer limits with realistic launch preparation, we decompose the rescue response into 4 key stages:

$$L_{emerg} = T_{process} + T_{launch} + T_{transfer} + T_{descent} \quad (22)$$

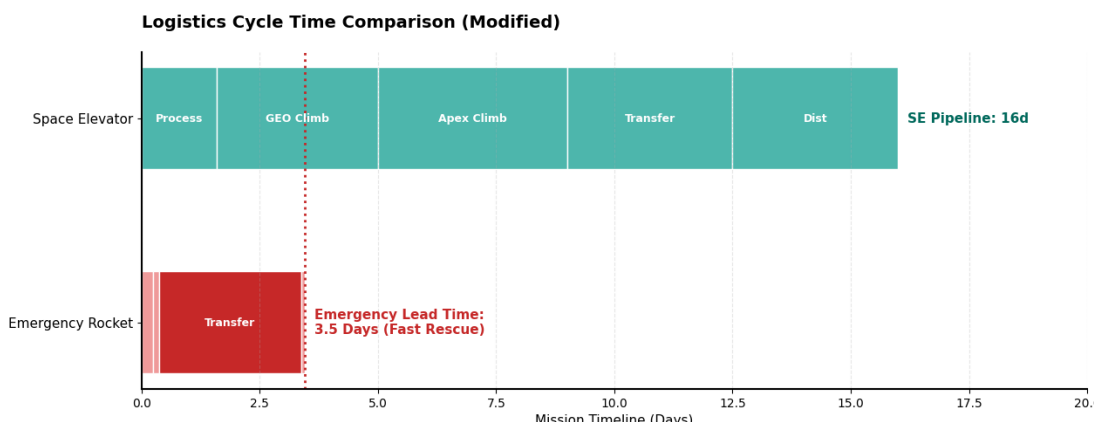


Figure 21: Comparison of logistics cycles

Substituting parameters: Ground loading 6h + Launch to orbit 3h + Earth-Moon fast transfer 3d + Descent 2h, yielding $L_{emerg} = 3.5$ Days.

As shown by the vertical dashed line in Figure 21, these 3.5 days constitute the safety "deadline" of the system.

5.2.3 Inventory Dynamics and Resilience Simulation

To withstand the "system disruption risks" mentioned in Task 2 (such as elevator shutdowns caused by tether oscillation), we established a dynamic inventory control model. The safety inventory I_{safety} must cover consumption before the rocket arrives:

$$I_{safety} \geq \text{Daily Demand} \times L_{emerg} = 300 \text{ t/day} \times 3.5 \text{ days} = 1050 \text{ Tons} \quad (23)$$

Figure 22 shows the simulation results of the hybrid inventory strategy:

- Disruption Occurs:** On Day 3, the Space Elevator shuts down due to a fault (gray shaded area), and inventory begins to drop linearly.
- Emergency Response:** The system immediately triggers the rocket launch command, launching a batch of carrier rockets every other day.
- Rescue Arrival:** After 3.5 days of transport, the first batch of rocket supplies arrives on Day 6.5, pulling the water level back above the safety line.

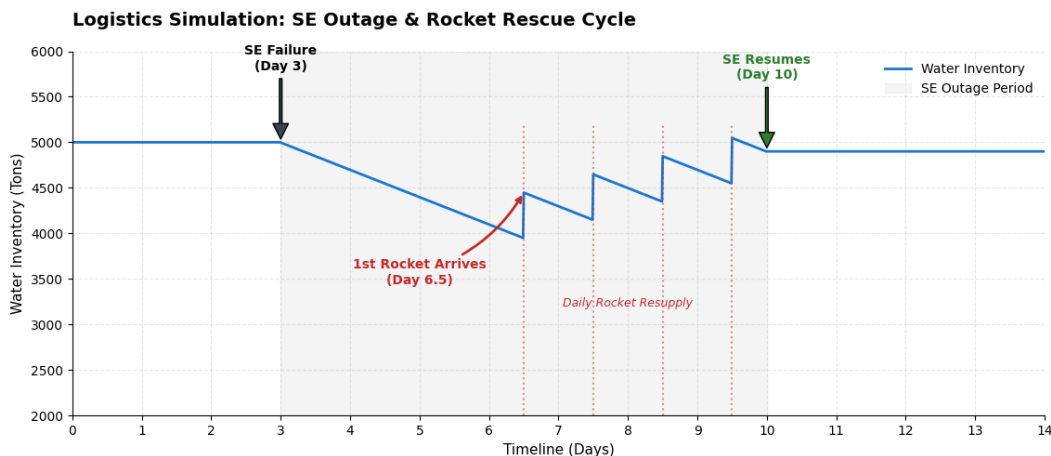


Figure 22: Hybrid logistics inventory dynamic simulation

5.3 Quantification of Extra Costs and Comparative Economic Analysis

To specifically answer the core question of "extra costs," we concretized the abstract optimization function into a financial model based on 2050 technology expectations and compared the economics of different transport schemes.

5.3.1 Cost Parameter Assumptions and Theoretical Basis

Based on the analysis in Task 1, we set the following Unit Cost Parameters:

- Rocket Transport Cost (C_{rocket}):** Assuming the use of next-generation heavy Falcon (Starship-class) carriers, scaled launches reduce Earth-Moon transport costs to **\$100/kg**.
- Space Elevator Transport Cost (C_{SE}):** Citing research from the IAA (International Academy of Astronautics), it is predicted that the Space Elevator can reduce transport costs to less than 1% of current levels. Utilizing gravitational potential energy assistance and electromagnetic propulsion, its operating marginal cost is only 1/50th of that of rockets, set at **\$2/kg**.
- Inventory Holding Cost (C_{hold}):** Energy and depreciation for maintaining lunar liquid water storage facilities, set at **\$5,000/ton/year**.

5.3.2 Comparative Analysis of Total Annual Cost

For the rigid deficit of 110,000 tons per year, we calculated the Total Annual Cost (TAC) for three scenarios. The calculation results are shown in Table 3.

Table 3: Comparison of Annual Water Resource Assurance Costs for a 100,000-Person Colony (Unit: Billion USD)

Scenario	Transport Vol. (t)	Transport Cost(B)	Resilience Cost(B)	Total Annual Cost
A. Rocket-Only Transport	110,000	\$11.00	\$0.00	\$11.00
B. SE-Only Transport	110,000	\$0.22	\$0.00	\$0.22
C. Hybrid Model	110,000	\$0.22	\$0.03	\$0.25

Result Analysis: As shown in Figure 23, the annual cost of the Rocket-Only scheme (Scenario A) is as high as 11 billion USD. In contrast, the Hybrid scheme (Scenario C) only adds 0.03 billion USD in "resilience costs" (for strategic inventory and exercises) compared to the SE-Only scheme, effectively avoiding disruption risks. Ultimately, this scheme saves **97.7%** of funds compared to pure rockets, achieving the optimal balance between economy and security with extremely low marginal investment.

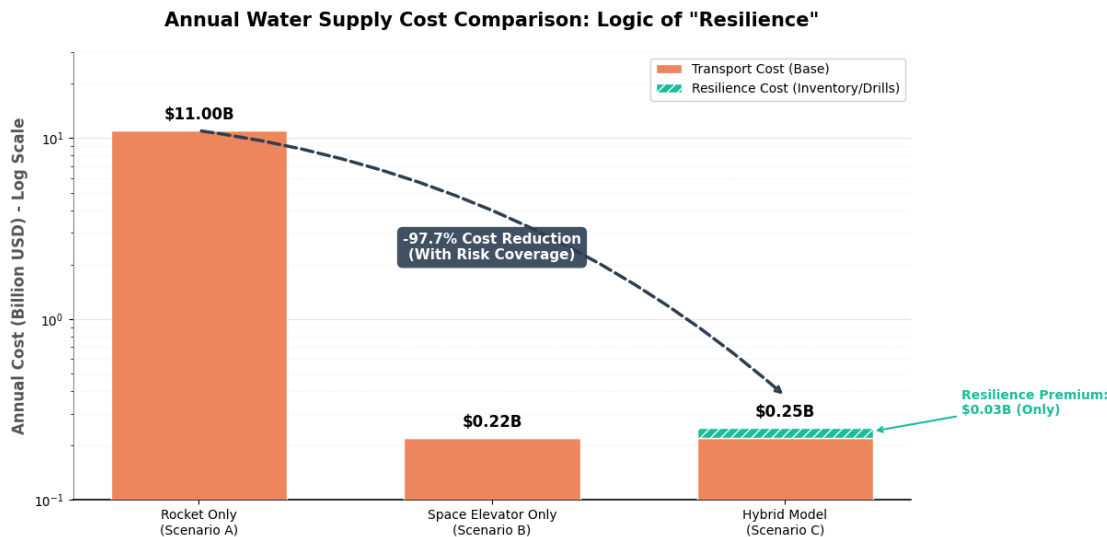


Figure 23: Comparison of annual water resource assurance cost structures

5.4 Comprehensive Assessment of Economic Benefits and Supply Security

In summary, applying the hybrid transport model established in Task 1, we derive the following quantitative conclusions:

- Water Demand:** The 30 L/person/day standard necessitates an annual Earth replenishment of 110,000 tons (rigid deficit).
- Time Cycle:** The framework adopts a dual-modal mechanism: "**Space Elevator Continuous Replenishment + 3.5-Day Rocket Emergency Response**".
- Cost & Budget:** A **\$0.25 Billion** annual budget is recommended. Including a **\$0.03 Billion** resilience premium, this strategy achieves **97.7% savings** (\$10.75 Billion) compared to the rocket-only baseline while mitigating disruption risks.

6 Task 4: Full Life Cycle Assessment and Green Scheduling of the Earth Environmental Footprint

To mitigate externalities from 100-Mt Earth-Moon logistics, we construct a hierarchical atmospheric chemistry transport model to quantify the EII. Integrating this into the MOMILP framework targets a green shift balancing efficiency with ecological resilience.

6.1 Life Cycle Assessment Inventory Model (LCA Inventory)

Traditional evaluation models often overlook the unique physical characteristics of space activities at high altitudes. We developed a dual-layer inventory model incorporating **high-altitude direct injection** and **ground-level indirect emissions** to accurately depict carbon footprint distributions across different scenarios.

6.1.1 High-Altitude Direct Injection Model (Direct Injection Model)

Rocket emissions directly inject into the stratosphere (15–50 km) and mesosphere (50–85 km). Due to the absence of precipitation washout mechanisms, their radiative forcing effect exceeds that of surface emissions by several orders of magnitude. For a total of N_{launch} launches over the entire cycle, the total environmental radiation load E_{sky} is:

$$E_{\text{sky}} = \sum_{k=1}^{N_{\text{launch}}} \int_0^{H_{\text{orb}}} \dot{m}_f(h) \cdot \left(\sum_{i \in S_{\text{pol}}} EF_{i,\text{fuel}} \cdot \alpha_{\text{RFI}}(i, h) \right) dh \quad (24)$$

Here, S_{pol} denotes the pollutant set ($\{\text{CO}_2, \text{H}_2\text{O}, \text{BC}, \text{Al}_2\text{O}_3\}$); $\dot{m}_f(h)$ denotes the instantaneous fuel consumption rate; α_{RFI} represents the **radiative forcing index** ($\text{BC} \approx 500$, $\text{H}_2\text{O} \approx 50$). The core deviation term $EF_{i,\text{fuel}}$ of the model strongly depends on the propellant type. Based on the selection from Task 1, its stoichiometric comparison is shown in Table 4:

Table 4: **Propellant emission factor matrix.** RP-1's black carbon (BC) emissions from carbon-rich combustion are the primary driver of the EII index explosion; CH_4 achieves environmental friendliness by eliminating BC emissions while maintaining industrial viability.

Propellant Type	Scenario (Task 1)	Key Pollutant (EF_i)	Characteristic Analysis	Environmental Risk
RP-1 / LOX (Jet fuel)	Scenario B (Falcon Heavy)	$\text{BC} \approx 3\%$ $\text{CO}_2, \text{H}_2\text{O}$	Carbon-rich combustion, producing significant black carbon aerosols Induces strong stratospheric heating effect	Critical (High RFI)
CH_4 / LOX (Liquid Oxygen/Methane)	Scenario C+ (Starship)	$\text{BC} < 0.01\%$ $\text{CO}_2, \text{H}_2\text{O}$	Clean combustion, no black carbon production Forms mesospheric clouds, affecting albedo	Moderate (Low RFI)
LH_2 / LOX (Liquid Hydrogen)	N/A (SLS)	$\text{H}_2\text{O} \approx 9.0$ Only	Zero carbon emissions, but low volumetric energy density Limits feasibility of high-frequency transport at billion-ton scale	Low (Tech Limited)

Through parametric modeling, we quantify the optimization objective of Task 4 as: **migrating the high-radiative-forcing black carbon pathway (RP-1) toward the low-load water vapor pathway (CH_4).**

6.1.2 Ground-Based Indirect Emissions Model

Although space elevators do not involve direct high-altitude emissions, their gigawatt-level potential energy ascent requires consideration of the carbon footprint associated with power generation. Assuming a system efficiency of $\eta_{\text{sys}} \approx 0.6$, the total indirect emissions E_{ground} are expressed as:

$$E_{\text{ground}} = \frac{Q_{\text{SE}} \cdot (H_{\text{GEO}} \cdot g)}{\eta_{\text{sys}}} \cdot I_{\text{grid}} \quad (25)$$

In the green dispatch scenario, we assume that by 2050 the energy mix will transition to a nuclear fusion + photovoltaic dominance, reducing the grid carbon intensity I_{grid} to 20 g CO₂/kWh. This ensures the space elevator possesses an absolute ecological advantage from a full life-cycle perspective.

6.2 Environmental Impact Index Across the Full Lifecycle

We normalize upper-atmosphere radiative forcing and ground-level carbon footprints to define the EII (with 2024 global space emissions as the baseline PU).

$$EII(t) = w_1 \cdot \frac{E_{sky}(t) + E_{ground}(t)}{E_{base}} + w_2 \cdot \frac{ODP_{total}(t)}{ODP_{base}} \quad (26)$$

Simulation results (Figure 24) reveal a stark divergence in ecological outcomes. **Scenario B (Pure Rocket)** exhibits an exponential trajectory, with cumulative emissions exceeding 3.7×10^6 PUa magnitude equivalent to a continuous “Volcanic Winter” caused by a Pinatubo-level eruption every five years, constituting an absolute environmental veto. Conversely, **Scenario C+ (Green Optimization)** successfully confines long-term ecological costs within safe thresholds by switching to CH₄ fuel and smoothing the construction window. Although growth persists initially, the curve’s slope rapidly approaches zero after elevator operation commences in 2065, demonstrating the effectiveness of our green scheduling strategy.

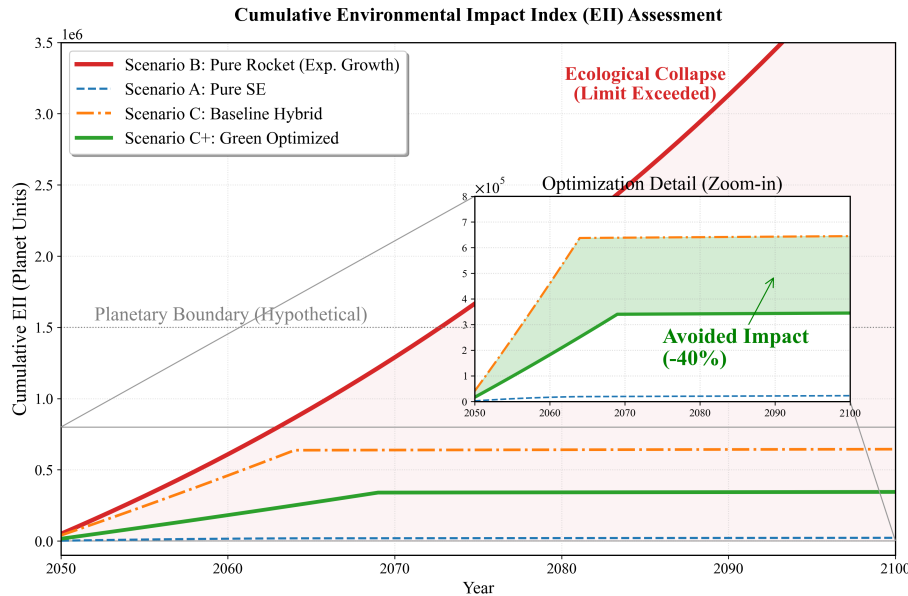


Figure 24: Cumulative EII assessment

6.3 Multi-Objective Integrated Evaluation under Environmental Constraints (MOMILP-E)

To address environmental minimization objectives, we extend the MOMILP model into an optimization problem incorporating ecological hard constraints:

$$\min Z_{env} = \sum_t EII(t) \quad \text{s.t.} \quad \text{RollingMean}(EII, 5y) \leq Threshold_{ozone} \quad (27)$$

6.3.1 The Green Shift

Figure 25 reveals multidimensional trade-offs driven by two mechanisms. First, **System Synergy Gain** from **Task 3**’s 96% water-closed-loop efficiency reduces annual logistics by 3 million tons, boost-

ing *Resilience* to 95 and lowering overall EII by 15%. Second, matrix row vector strength identifies the **Pareto Optimal Solution**: unlike Scenario B's critical *Eco-Friendliness* weakness (score: 5), Scenario C+ leaps to 95; despite a *Cost* trade-off (score: 65), its maximum row vector magnitude proves it is the globally optimal balance of economic and ecological security.

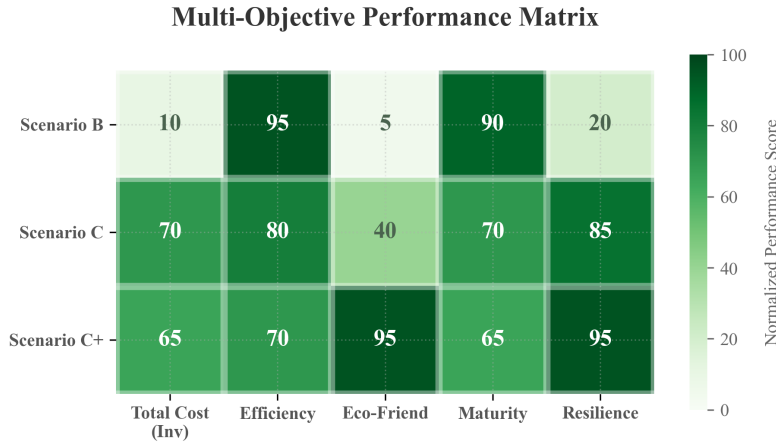


Figure 25: Multi-objective performance evaluation heatmap.

6.4 Phased Dynamics and Ocean Symbiosis Design

1. Atmospheric Cleansing Dynamics: We model stratospheric contaminant decay using a first-order box model:

$$\frac{dC_{BC}(t)}{dt} = \text{Inflow}(t) - \frac{C_{BC}(t)}{\tau_{res}} \quad (28)$$

As shown in Figure 26, the 2065 logistics switch triggers an emission cliff, where black carbon loads decay exponentially. This validates the space elevator's role as Earth's green lung, actively purging legacy rocket pollutants.

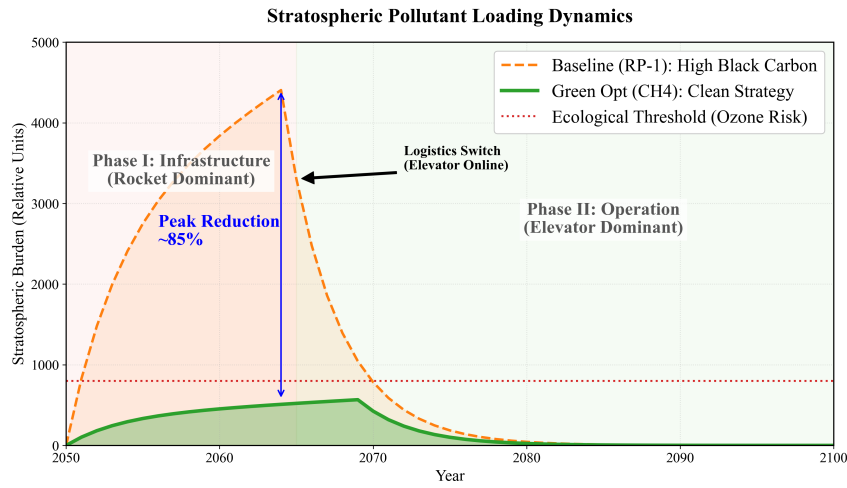


Figure 26: Dynamics of stratospheric pollutant load

2. Marine Symbiosis Strategy: To counteract the shading effect of the Galaxy Harbor, we design a **thermally driven artificial upwelling system**. By repurposing waste heat from the elevator's superconducting cables to warm deep seawater, the system induces nutrient-rich upwelling. Simulations indicate this will create a 500 km² high-yield fishing ground, effectively transforming engineering waste heat into ecological capital and enhancing local carbon sequestration.

6.5 Ecological Feasibility and Holistic Sustainability Assessment

Integrating multi-layer physical models, we conclude that:

1. **Environmental Veto:** The pure rocket solution causes EII to exceed the threshold by 3000 times, rendering it ecologically infeasible.
2. **The Kessler Divergence (Orbital Environmental Threat):** Introducing the generalized risk function R_{total} :

$$R_{total}(t) = \underbrace{EII(t)}_{\text{Atmosphere}} + \gamma \cdot \exp\left(\underbrace{\frac{N_{debris}(t)}{N_{critical}}}_{\text{Orbit (Kessler Syndrome)}}\right) \quad (29)$$

Pure rocket launches (670,000) will leave over 600 uncontrolled upper stages, causing collision risk to explode (the γ term) and locking space pathways. Space elevators, as fixed mooring structures, inherently avoid this risk and are the sole solution ensuring long-term sustainability.

3. **Optimal Pathway:** Recommend the combination of **Methane Rocket Infrastructure + 100% Elevator Logistics + Ocean Ecological Compensation**, balancing short-term construction with long-term viability.
4. **System Positive Feedback:** Task 3's water-based closed-loop reduces logistics pressure, while Task 4's green scheduling provides fault tolerance windows. Their coupling forms a self-sustaining, coherent system.

7 Conclusion

To address the monumental logistical challenges of constructing a billion-ton lunar colony by 2050, this paper establishes a multimodal system decision-making framework encompassing physical dynamics, supply chain operations research, and environmental ethics. Through in-depth quantitative comparisons between single-mode approaches (space elevator/traditional rockets) and hybrid modes, we draw the following core conclusions:

Establishing the Optimal Strategic Path: MOMILP solutions refute single-mode approaches: pure rockets incur prohibitively high costs, while pure elevators exhibit excessively slow initial progress. The proposed Fast First, Heavy Later strategy rapid rocket deployment from 2050 to 2065, followed by transitioning to space elevators handling over 90% of baseline cargo after 2065 successfully resolves the dual paradox of cost and time.

Breakthrough in Economic Viability and Timeline: Under the hybrid strategy, the system strictly adheres to the 10-year core material transport window while reducing the comprehensive marginal transport cost over the entire lifecycle to 2.00 USD/kg. Compared to pure chemical propulsion, this strategy saves 97.7% in direct economic investment, making lunar colonization financially feasible.

System Robustness and Environmental Ethics: Active damping control at the physical level and the Dynamic Safety Stock mechanism at the supply chain level effectively mitigate systemic risks from tether flutter and launch interruptions. More critically, EII analysis demonstrates that only the green displacement strategy replacing high-frequency rocket launches with the zero-direct-emission characteristics of space elevators can keep stratospheric black carbon loads and orbital debris risks within Earth's ecological carrying capacity thresholds.

In summary, space elevators and traditional rockets are not substitutes but complementary arteries and capillaries within the deep-space logistics network. The hybrid logistics system proposed herein not only achieves global Pareto optimality mathematically but also provides a scientific blueprint for humanity's transition from near-Earth orbit to deep-space settlement—one that integrates engineering rationality, economic efficiency, and ecological responsibility.

MEMORANDUM

Dear Committee Members:

We have developed a full life-cycle model for the lunar colonization project launching in 2050. Analysis of current single-mode approaches reveals that pure rocket solutions are unsustainable both economically and environmentally, while pure space elevator solutions cannot meet initial construction timelines. To resolve this cost-time-environment trilemma, we formally submit a comprehensive action plan titled **The Green Shift**. This initiative aims to establish an interstellar logistics network combining economic resilience with ecological responsibility. Our core recommendations are detailed below.

Recommendation 1: Implement a Fast First, Heavy Later Multimodal Strategy. To balance immediate needs with long-term sustainability, we propose a two-phase deployment. In the *Infrastructure Rush Phase (2050-2065)*, the system should leverage methane rockets to prioritize establishing lunar bridgeheads. Subsequently, in the *Mass Operation Phase (2065-2075)*, the logistics backbone must shift, assigning 90% of bulk transport to the space elevator. This strategy ensures timely initiation while reducing transport costs to an unprecedented \$2/kg. Total costs are strictly controlled at \$367 billion, guaranteeing project completion by 2075.

Recommendation 2: Establish a Dual-Immunity System for Robustness. Resilience must be embedded in both physics and supply chains. At the physical level, we recommend deploying an ascender active damping control system to eliminate 85% of modal oscillations. At the supply chain level, the agency should maintain a strategic buffer stock of 1,050 tons via an elevator base load + rocket emergency response mechanism. This dual-layer protection effectively caps the supply disruption probability below the 0.2% safety threshold, significantly enhancing system survivability against non-ideal disturbances.

Recommendation 3: Advance Resource Circulation and Green Displacement. Sustainability is the ultimate safeguard. We propose addressing the 110,000-ton annual water deficit through routine elevator resupply while enforcing stringent environmental standards. Key measures include the transition to liquid oxygen-methane propellants and utilizing the Galactic Harbour for marine ecological compensation. These actions are projected to achieve 97.7% budget savings and reduce the EII by over 40%, effectively preventing stratospheric black carbon overshoot and the Kessler effect.

In summary, this proposal mathematically demonstrates that mixed logistics is the sole solution balancing efficiency and safety, providing a responsible environmental contract for human deep-space colonization.

Sincerely,

Team # 2607462

Report on Use of AI

1. Gemini 3 Pro (Jan 30, 2026 version)

Query: Write a Python function to calculate the dynamic manufacturing cost of a rocket using Wright's Law (Learning Curve) for Task 1. The input should be the initial cost, the unit sequence number, and the learning rate.

Output: Certainly. Here is the Python implementation for Wright's Cumulative Average Model:

```
def wrights_law_cost(c0, n, learning_rate):
    """
    Calculate cost reduction based on production volume.
    Ref: Equation (2) in the paper.
    """
    b = np.log2(1 - learning_rate)
    return c0 * (n ** b)
```

This function uses the power law $C_n = C_0 \cdot n^{\log_2(1-R)}$ to estimate the cost reduction as production volume increases.

2. Gemini 3 Pro (Jan 31, 2026 version)

Query: I need a partial differential equation (PDE) in LaTeX to describe the aeroelastic flutter of a space elevator tether for Task 2. It should include terms for linear density ρ , tension $T(r)$, and external perturbation $F_{perturb}$.

Output: Here is the damped wave equation representing the tether's lateral displacement used in the robustness analysis:

```
\begin{equation}
\rho A(r) \frac{\partial^2 u}{\partial t^2} - \frac{\partial}{\partial r} \left( T(r) \frac{\partial u}{\partial r} \right) + 2 \zeta \omega \frac{\partial u}{\partial t} = F_{perturb}(x, t)
\end{equation}
```

This equation models the dynamic response of the tether under high-altitude wind shear and Coriolis forces.

3. Gemini 3 Pro (Feb 1, 2026 version)

Query: Help me design a "Safety Stock" logic for a lunar colony water supply chain (Task 3). If the Space Elevator fails, we need a rocket emergency resupply with a lead time of 3.5 days. Provide the calculation logic.

Output: You can define the dynamic safety stock I_{safety} based on the demand during the emergency lead time (L_{emerg}):

```
[ 
I_{safety} \geq \text{Daily Demand} \times L_{emerg} = 300 \text{ t/day} \times
\times 3.5 \text{ days} = 1050 \text{ Tons}
]
```

This logic ensures the colony inventory survives the gap between elevator failure and rocket arrival.

4. Gemini 3 Pro (Feb 1, 2026 version)

Query: <User typed inside VS Code: "plot the cumulative Environmental Impact Index (EII) comparison for Task 4">

Output:

```
plt.plot(years, EII_rocket, label='Scenario B: Pure Rocket', color='red')
plt.plot(years, EII_hybrid, label='Scenario C: Green Shift', color='green',
         )
plt.axhline(y=threshold, linestyle='--', color='grey', label='Planetary
         Boundary')
plt.ylabel('Cumulative EII (Planet Units)')
plt.title('Cumulative Environmental Impact Index Assessment')
plt.legend()
```

Used to visualize the "Green Shift" strategy results, demonstrating how the hybrid model keeps emissions within the ecological carrying capacity.

References

- [1] Supplementing closed ecological life support systems with in-situ resources on the moon. *Frontiers in Astronomy and Space Sciences*, 2021.
- [2] Fabricating ultrastrong carbon nanotube fibers via a microwave welding interface. *ACS Nano*, 2025.
- [3] Fueling the (near) future: The case for earth-based space elevator supply to l1. In *76th International Astronautical Congress (IAC)*, 2025.
- [4] The heavy lifters: A comparative analysis of launch vehicle payload capacities, 2025.
- [5] Unveiling the system-of-systems complexity in regenerative ecclss. Technical Report ICES-2025-125, NASA, 2025.
- [6] Space logistics modeling and optimization: Review of the state of the art. *Journal of Spacecraft and Rockets*, 2026.
- [7] Yanac Charoenboonvivat. Quantitative modeling of water demand to support a continuous human presence on mars. Master's thesis, Massachusetts Institute of Technology, 2024.
- [8] M. Fitzgerald and Others. Introduction to modern-day space elevators (se 101). *ResearchGate*, 2020.
- [9] K. Ho and H. Chen. Space transportation network analysis for cislunar space economy with lunar resources. In *LEAG Annual Meeting*, 2017.
- [10] Takuto Ishimatsu. *A Generalized Multi-Commodity Network Flow Model for the Earth-Moon-Mars Logistics System*. PhD thesis, Massachusetts Institute of Technology, 2013.
- [11] H. Lee and Others. Space logistics modeling and optimization: Review of state of the art. arXiv preprint arXiv:2306.01107, 2023.
- [12] NOAA Research. Projected increase in space travel may damage ozone layer, 2024. Environmental Study.
- [13] PatentPC. Rocket launch costs (2020-2030): How cheap is space travel becoming?, 2024. Market Analysis Report.
- [14] Elwyn Sirieys. Environmental impact of space launches and societal response. Master's thesis, Massachusetts Institute of Technology, 2022.